Thermal crosstalk measurements and simulations for an X-ray microcalorimeter array

Poster n°81

Antoine R. Miniussi [a], [b], Joseph S. Adams [a], [b], Simon R. Bandler [a], Sophie Beaumont [a], [b], Meng P. Chang [a], [c], James A. Chervenak [a],
Fred M. Finkbeiner [a], [d], Jong Y. Ha [a], [e], Ruslan Hummatov [a], [b], Richard L. Kelley [a], Caroline A. Kilbourne [a], Frederick S. Porter [a],
John E. Sadleir [a], Kazuhiro Sakai [a], [b], Stephen J. Smith [a], [b], Nicholas A. Wakeham [a], [b], Edward J. Wassell [a], [c]

Contact : antoine.r.miniussi@nasa.gov

Abstract

Arrays with high-density microcalorimeters need sufficient heatsinking in order to minimize the thermal crosstalk between nearby pixels. For the array of superconducting transition-edge sensors (TES) developed for the Athena/instrument, which has more than 3000 pixels on a very fine 275 µm pitch, it is essential to address this problem. The mission requires the impact of the thermal crosstalk on the energy resolution to be less than 0.2 eV. This value results in a secondary requirement that the ratio between the amplitude of the crosstalk signal to the 6 keV pulse is less than 1e-3 (for the first neighbor), 4e-4 (for the diagonal neighbor) and 8e-5 (for the second neighbor). We have measured the thermal crosstalk levels between pixels in various geometries and configurations. The results show a crosstalk ratio which is at least a factor of 4 lower than the secondary requirement. We also developed a FEM 2D thermal model to predict thermal behavior of large-scale arrays. This model successfully simulates the measured data in terms of pulses amplitude and time constants.

Experimental setup for crosstalk measurements

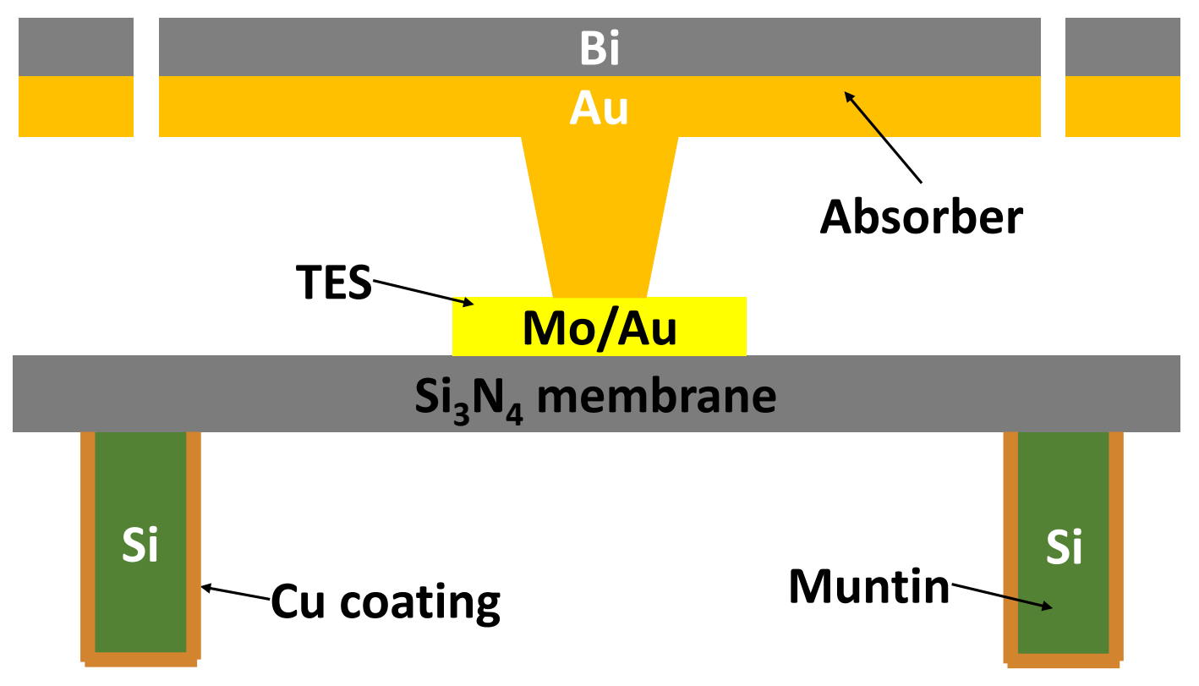

Diagram of the TES side

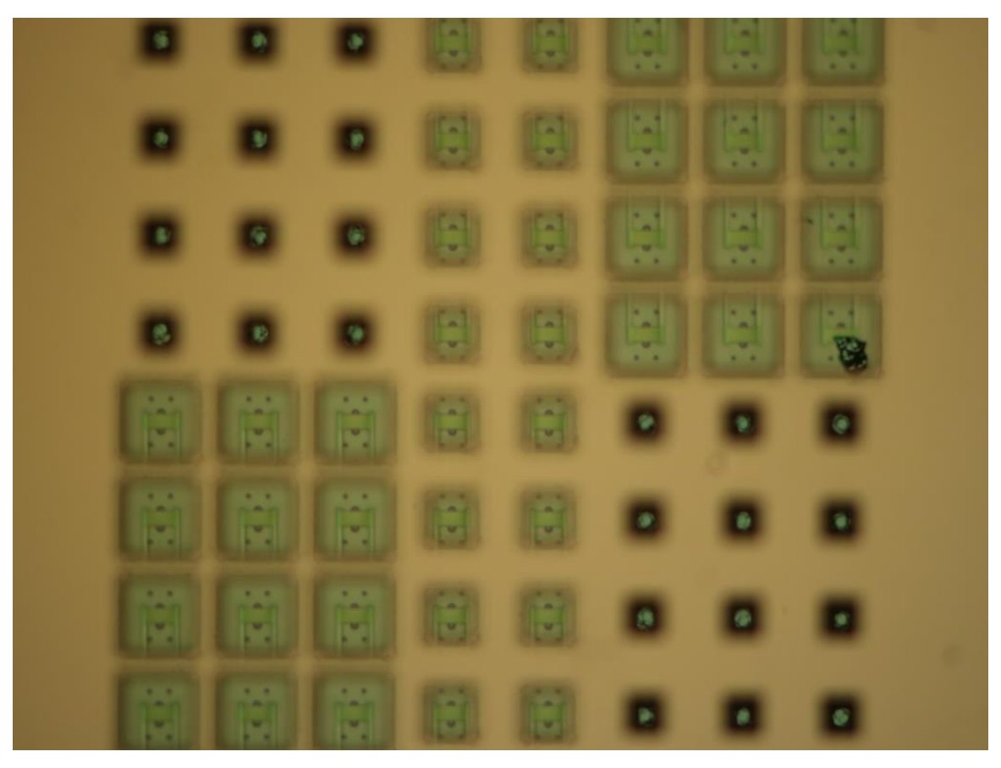

Bottom view of the TES array

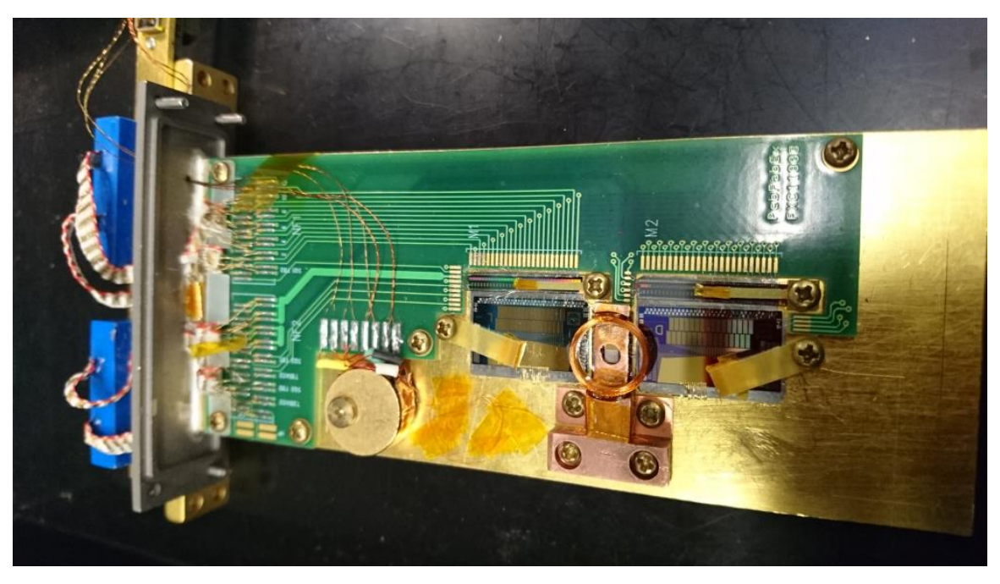

Experimental setup card

Main components:

- Mo/Au superconducting **Transition Edge Sensor** (TES) detector: 75 µm wide, aspect ratio of 1:0.5
- Bi/Au absorber: 240 µm for a 250 µm pitch. The pitch may increase the for Athena/X-IFU instrument
- Si_3N_4 membrane: uniform over the array, it supports the TES and its absorber
- Si muntins: supports the Si3N4 membrane around each TES and acts as a heatsink
- Cu coating: covers the sides and the bottom of the muntins to improve thermal conductivity

Two 8x8 arrays tested:

- Chip A: 5 different muntin widths of **42 µm**, **77 µm**, **112 µm**, 130.5 µm and 149 µm (middle picture)
- Chip B: uniform chip with muntins width of **112 µm** and **105 µm** on the orthogonal direction.
  Measurement done before and after adding the Cu coating on the backside of the chip

Cryogenics and readout

- ADR cryogenics system running at bath temperature of 55 mK
- X-ray emitted by 55Fe source at 5.9 keV

Measurements

Each measurement implies two selected TES, one defined as the "***source***", the other one as the "***receiver***"

- Measurement triggered when the *source* is hit by 5.9 keV X-ray
- *Receiver* signal is saved for each trigger (> 4000 samples)
- Data set is recorded for positive and negative TES bias points of the receiver (electrical crosstalk)
- 5.9 keV pulse hits are recorded for the *receiver* at same bias point

Data processing

- Data sets are averaged to get better S/N ratio
- Electrical crosstalk is removed by subtraction of the *receiver* positive and negative bias point data sets
- Maximum of the 5.9 keV pulse on *receiver* is calculated by fitting a single exponential equation to discard non-linearity effect of the TES. Amplitude is defined as $\mathbf{h_{6keV}}$
- Maximum of the crosstalk signal on *receiver* is calculated by averaging 20 points. Amplitude is defined as $\mathbf{h_{crosstalk}}$.
- Rise and decay time constants are measured for each crosstalk pulse
- We introduce a figure of merit, the crosstalk ratio $f = \frac{h_{crosstalk}}{h_{6keV}}$

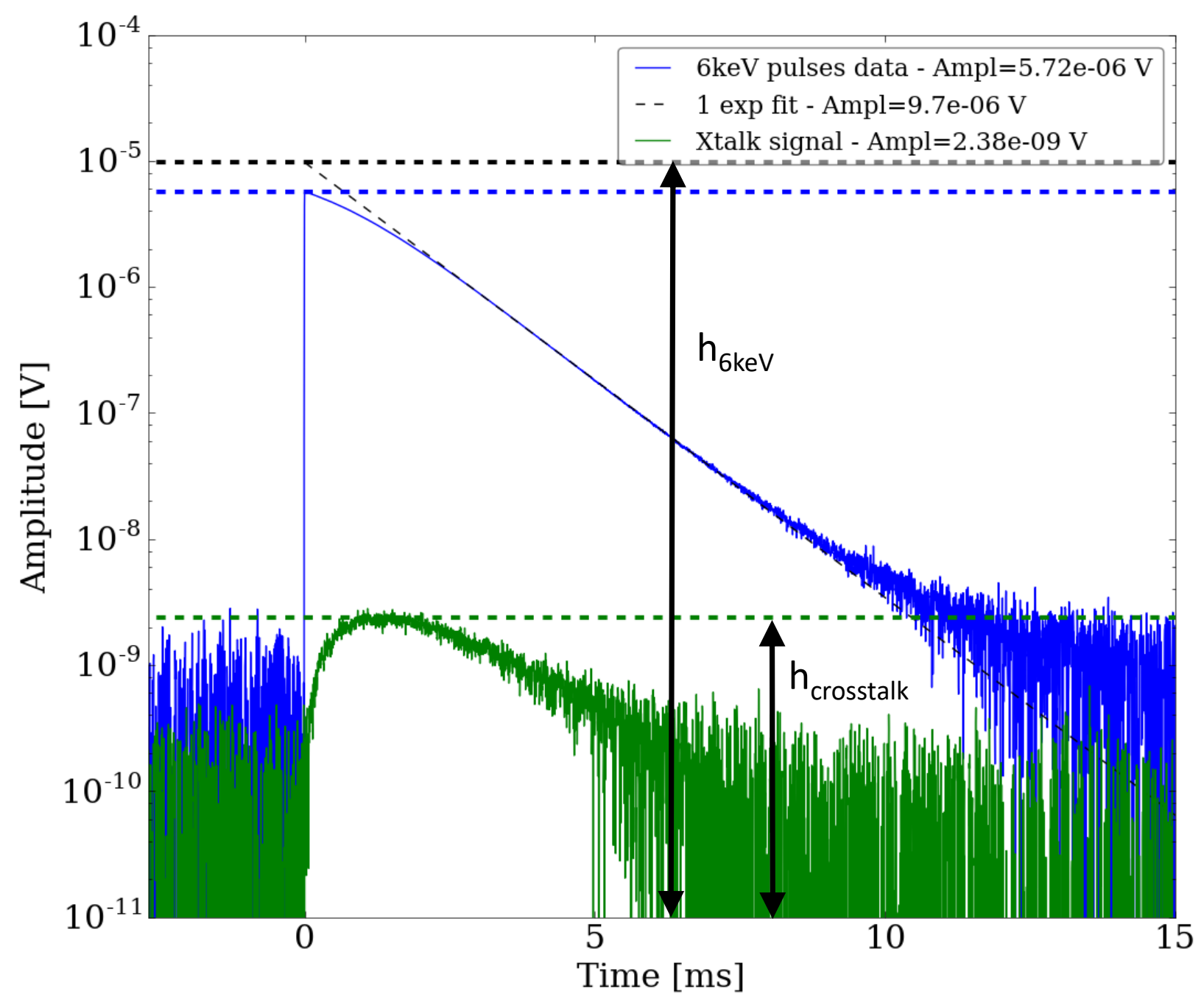

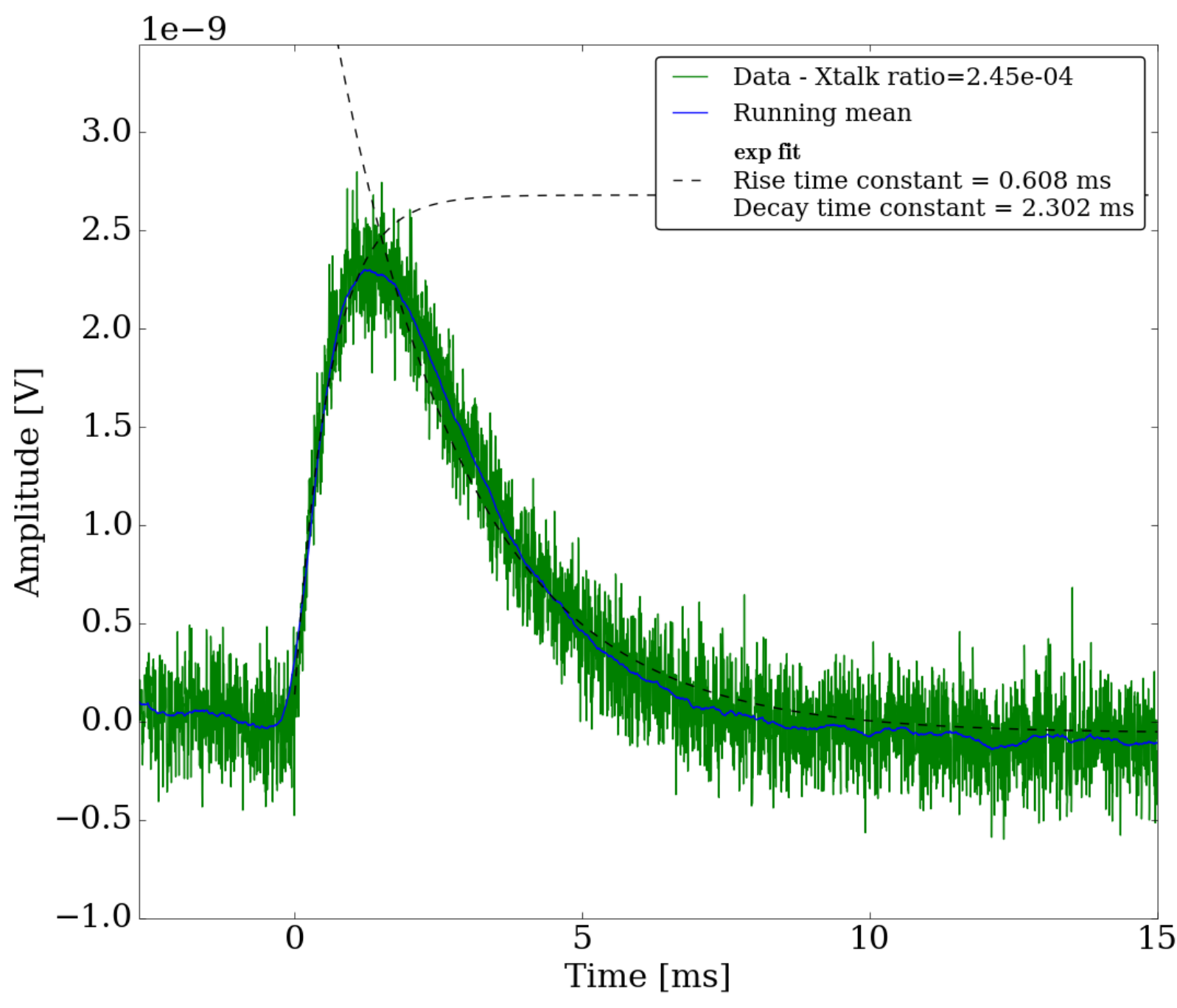

Experimental results

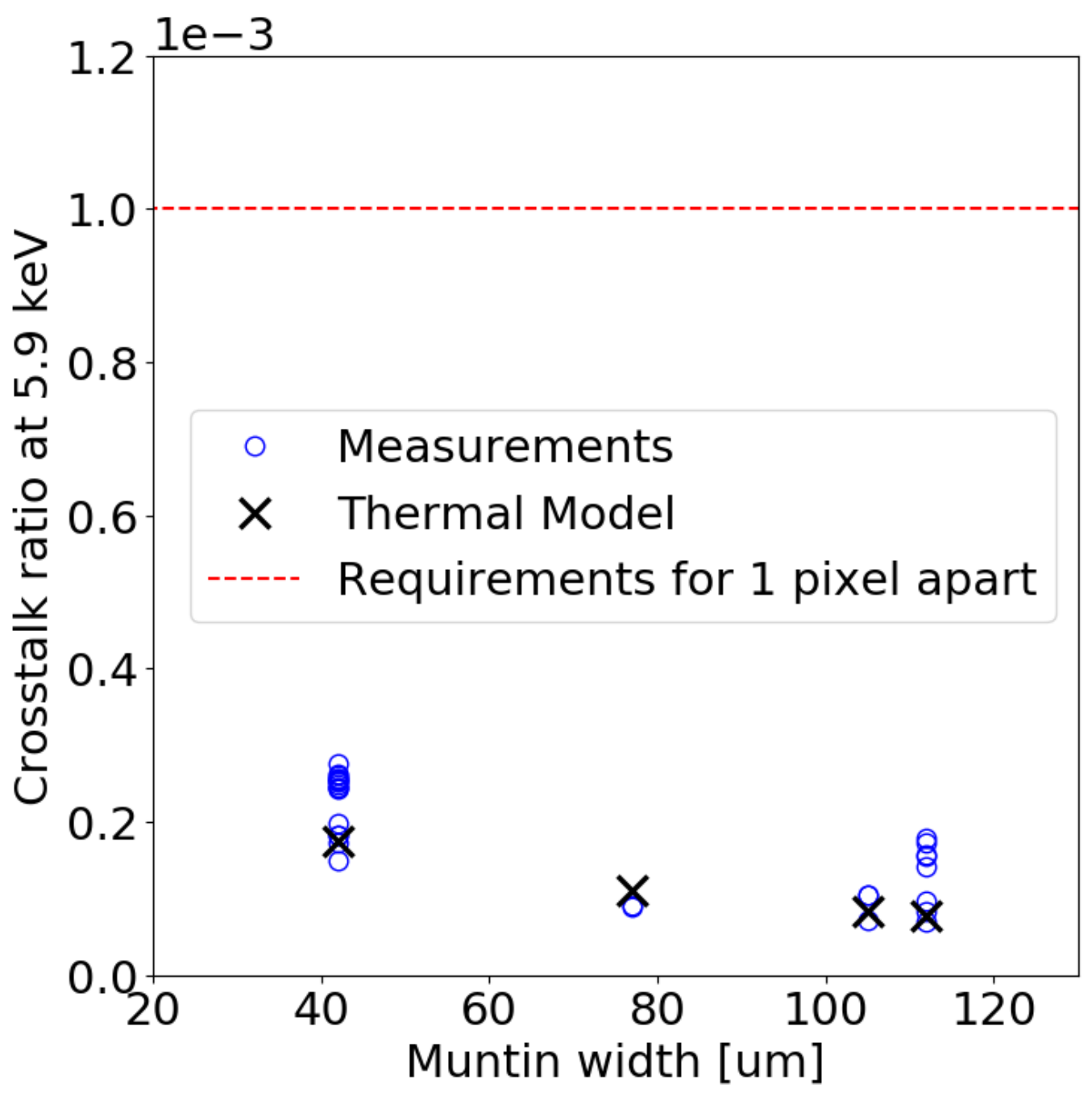

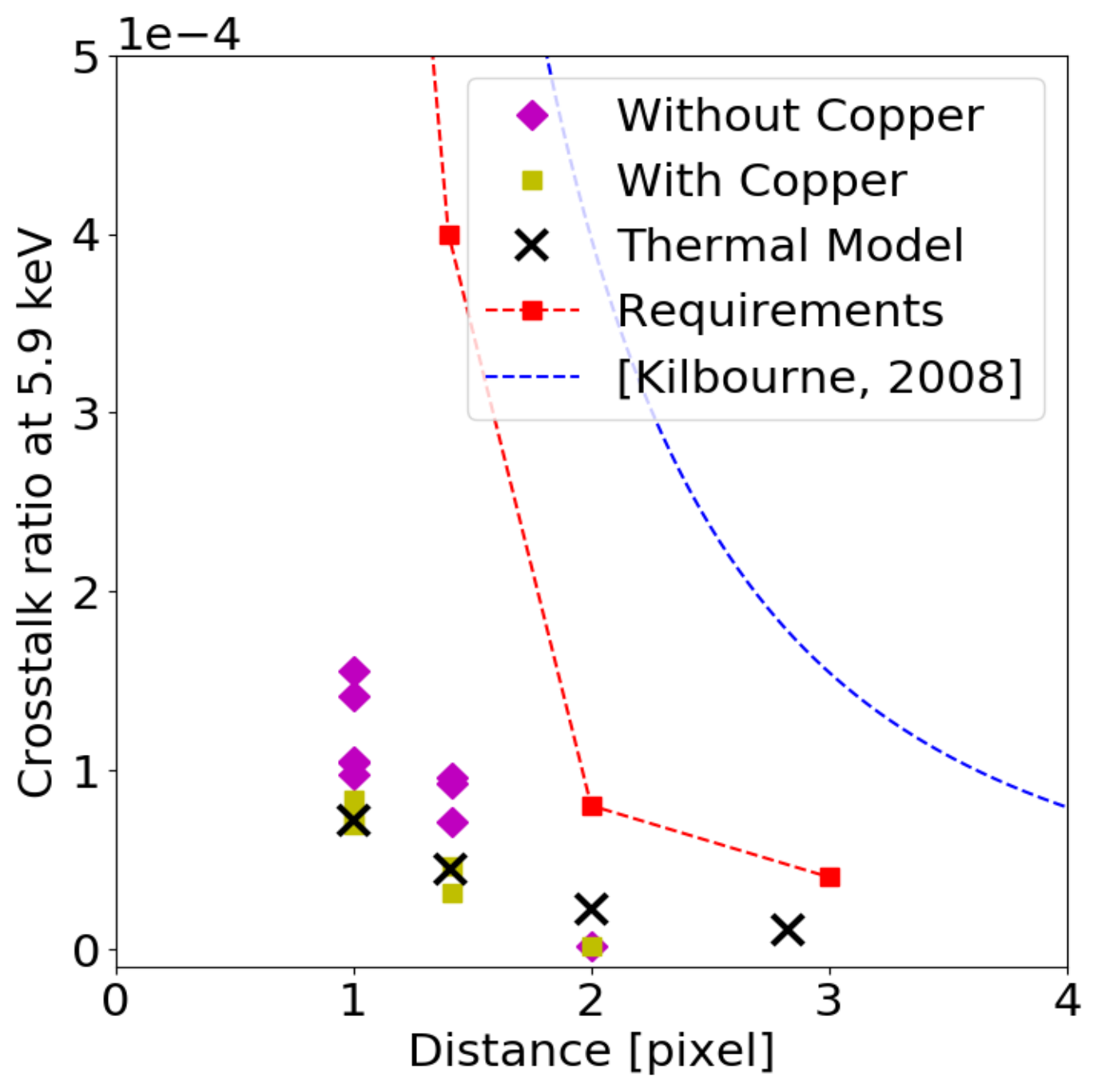

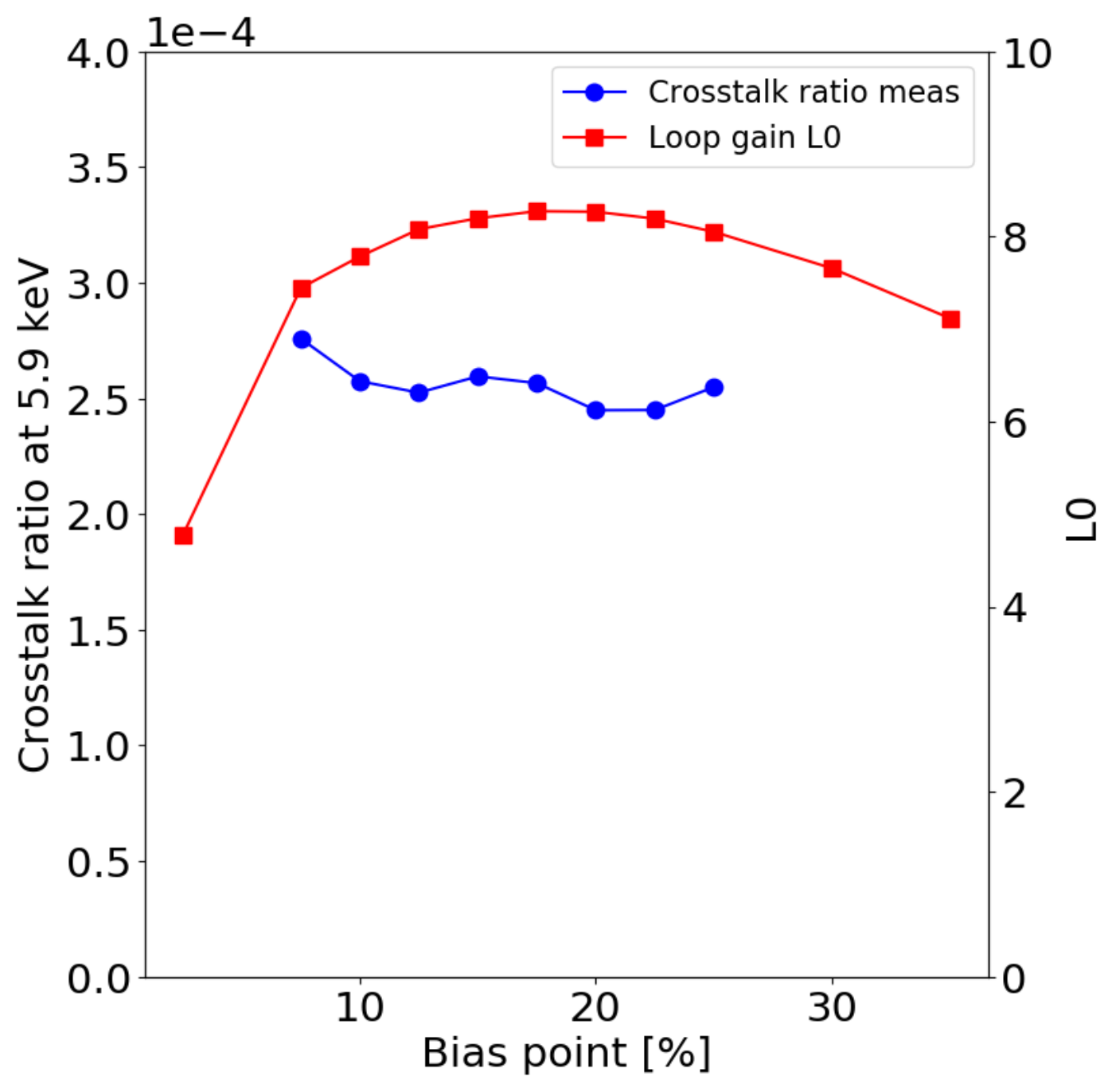

Crosstalk ratios as function of muntin width for nearest pixel

- Crosstalk ratio stays below the requirements
- Increasing the muntin width decreases the crosstalk ratio
- Results are similar for day to day measurement of when swapping *source* and *receiver* TESs

Crosstalk ratios as function of distance for 112 µm muntin width

- Crosstalk ratio decreased compare to previous measurements [Kilbourne, 2008] for 70 µm muntin width. The difference can be explained by a higher loop gain, larger muntin width or the removal of the passivation layer.
- Stays below the requirements by a factor 4 or more for all positions
- Cu on the backside of the TES decreases the crosstalk ratio by 50% in the case of 8x8 array

Crosstalk ratios as function of bias point for 42 µm muntin width

- Crosstalk ratio is constant over the whole range of bias points with variation within 5%
- The loop gain L_0 doesn't impact the results since it stays constant over the range of bias points studied

Requirements

The Athena/X-IFU mission has allocated 0.2 eV within the energy-resolution budget for thermal crosstalk, this results in the following secondary requirements:

- Thermal crosstalk ratio f lower than 1e-3 (for the first neighbor), 4e-4 (for the diagonal neighbor) and 8e-5 (for the second neighbor)

Numerical model - Validation

A numerical thermal model has been developed to understand thermal crosstalk and predict the impact of future changes of the TES array design. The model is developed in 2D under the Finite Element Method (FEM) software Comsol Multiphysics. It is composed of 4000 elements.

Five blocks are modeled: Pixel, Si, electron and phonon components of the Cu coating and the heatsinking. The loop gain with its factor L_0 is implemented through a change of the heat capacity of the pixel.

Thermal parameters:

- Constrained C_{pixel} and G_{bath} (measured)
- Floating and with high impact: Gelectron-phonon, Gkapitza_Si-Cu and Gwb
  All the values stay within the error bars observed in the literature

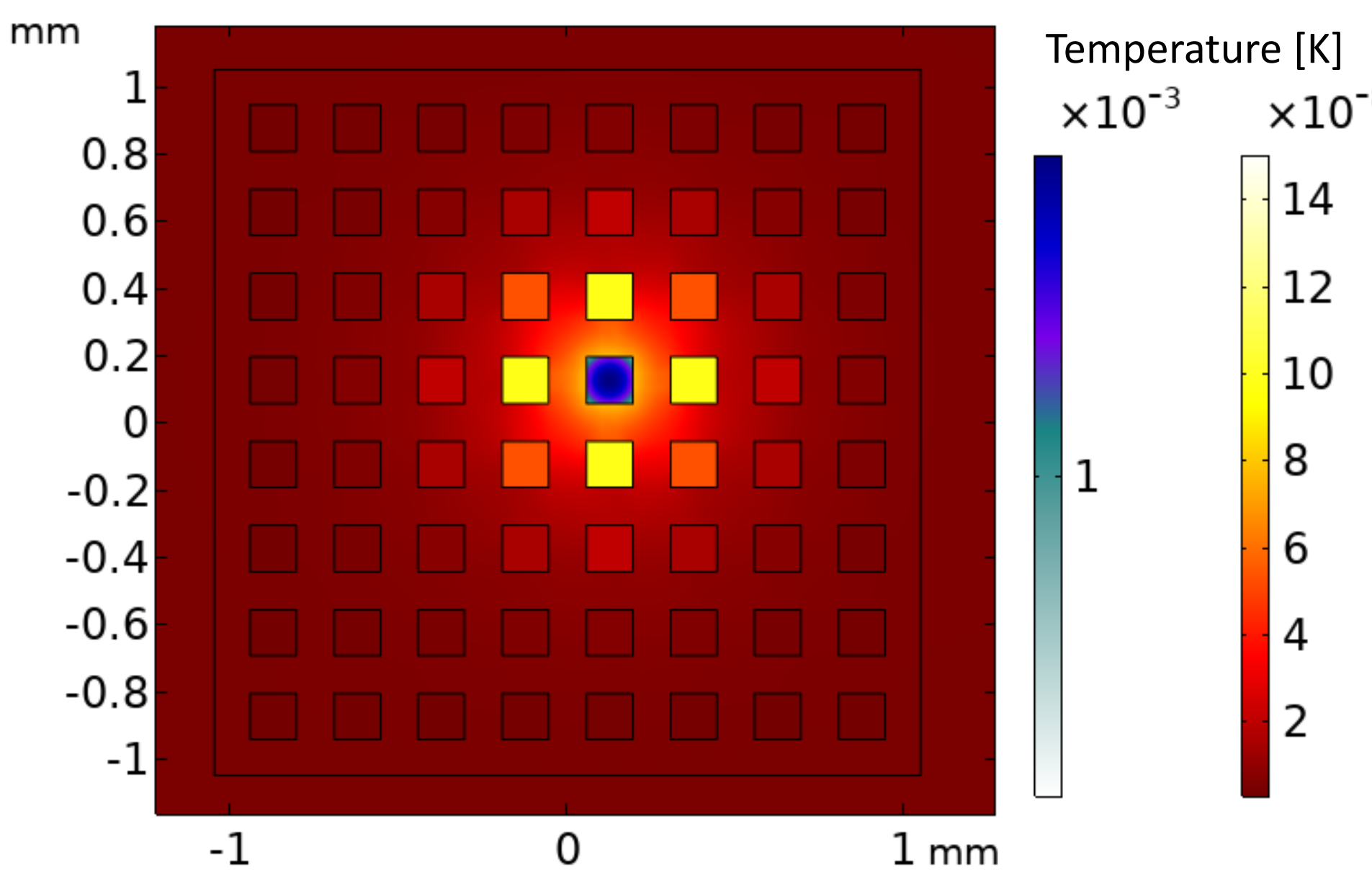

Modeled temperature elevation for the whole array

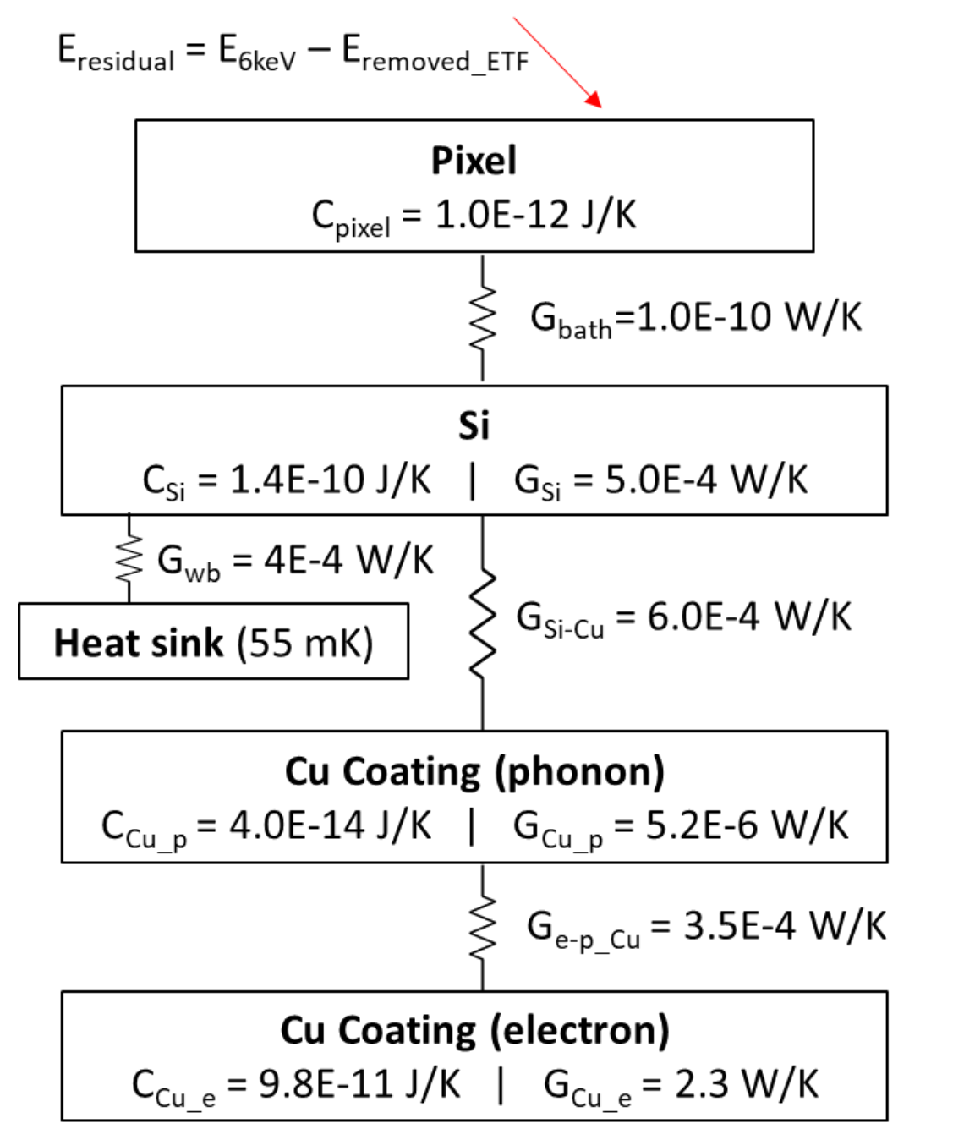

$E_{residual} = E_{6keV} - E_{removed\_ETF}$

Pixel
C_{pixel} = 1.0E-12 J/K

G_{bath}=1.0E-10 W/K

Si
C_{Si} = 1.4E-10 J/K | G_{Si} = 5.0E-4 W/K

G_{wb} = 4E-4 W/K

Heat sink (55 mK)

$G_{Si\text{-}Cu}$ = 6.0E-4 W/K

Cu Coating (phonon)
C_{Cu_p} = 4.0E-14 J/K | G_{Cu_p} = 5.2E-6 W/K

$G_{e\text{-}p\_Cu}$ = 3.5E-4 W/K

Cu Coating (electron)
C_{Cu_e} = 9.8E-11 J/K | G_{Cu_e} = 2.3 W/K

Results:

The numerical thermal model is run for all the geometries for a loop gain L_0=8 and always includes the Cu coating.

➔Model results are compared to data on the 2 plots in left of this poster (black crosses)

➔The **model shows a very good accuracy**:

- Crosstalk ratio has a maximum error of 20% for muntin widths of 42 and 112 µm
- Rise (~ 0.7 ms) and decay (~ 2.5 ms) time constants have a maximum error of 20 %

Plots: Comparison between the measured and simulated signals of the 6 keV pulse (yellow) and the crosstalk pulses for different configurations.

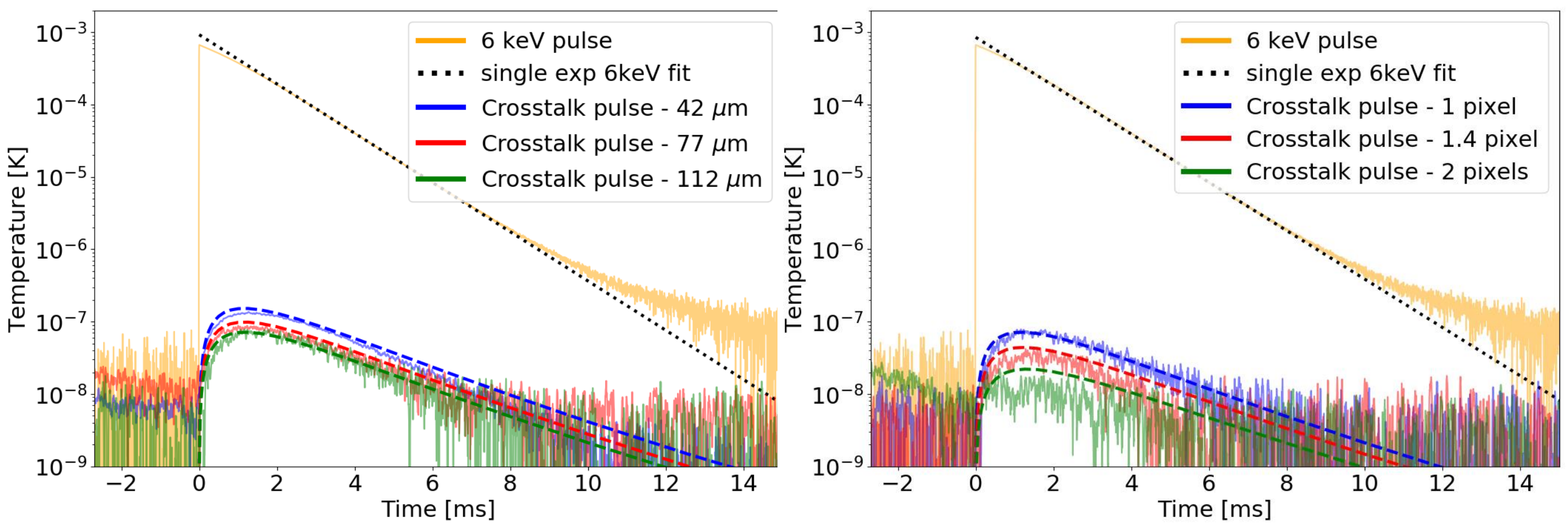

Comparison between measurements (solid line) and results from thermal model (dashed line) for 3 different muntin widths (**right**) and 3 distances (**left**). The dot line represents the fitted measured 6 keV pulse. The measured data, in nV, are normalized in order to get the maximum of the fitted 6 keV pulse at 1 mK.

Conclusions and future work

Experimentation

➔ Crosstalk ratio is at least 4 times lower than requirement for 1 or more pixel apart

➔ Increasing the muntin width decreases the crosstalk

➔ Adding a coating layer of Cu improves the crosstalk by 50% for this small chip

Model

➔ The numerical model fit the experiment data with a 20 % error on the crosstalk ratio and the rise and decay time constants

➔ Implement the ETF response in the model

Future work

➔ Further measurements at higher bias point (lower L_0)

➔ Define the impact of a change of inductance on the crosstalk ratio

➔ Studying the impact of the thermal crosstalk on the energy resolution

➔ Model the future Athena/X-IFU array to predict the thermal crosstalk impact

Affiliations

[a] : NASA Goddard Space Flight Center
[b] : CRESST II – University of Maryland Baltimore County
[c] : SSAI Science Systems and Applications, Inc.
[d] : Sigma Space Corp.
[e] : SB Microsystems

18th international Workshop on Low Temperature Detectors – July 2019